Appl. Phys. B 75, 385–389 (2002)
DOI: 10.1007/s00340-002-0972-y

Applied Physics B
Lasers and Optics

D. COSTOPOULOS
A. MIKLÓS
P. HESS✉

Detection of N_2O by photoacoustic spectroscopy with a compact, pulsed optical parametric oscillator

Institute of Physical Chemistry, University of Heidelberg, Im Neuenheimer Feld 253, 69120 Heidelberg, Germany

Received: 29 April 2002/Revised version: 4 June 2002
Published online: 21 August 2002 •

ABSTRACT A pulsed optical parametric oscillator (OPO) operated in an optical cavity with a grazing-incidence grating configuration (GIOPO) was used for sensitive photoacoustic detection of trace quantities of dinitrogen oxide (N_2O). The ($\nu_1 + \nu_3$) combination vibration band of N_2O was excited with the idler beam of the GIOPO at 2.86 μm using an optical cavity optimized for the idler beam. The linewidth of the GIOPO could be reduced to 0.4 cm^{-1}, allowing the rotational structure of the absorption spectrum to be resolved. A concentration sensitivity (signal-to-noise ratio = 3) of 60 parts in 10^9 by volume (60 ppb V) N_2O in synthetic air was obtained. This may be sufficient for continuous monitoring of N_2O in the atmosphere.

PACS 42.62.Fi; 42.65.Yj; 07.07.Df; 42.68.Ca

1 Introduction

Molecule-specific detection and real-time monitoring of trace amounts of nitrogen oxides are not only important for monitoring changes in the atmosphere ("nitrogen cycle") [1] but also in other fields, such as agriculture, medicine, and biology [2]. Nitrous oxide (laughing gas) has been found to be one of the most effective greenhouse gases, due to its strong absorption in transmission regions of the atmosphere. According to recent studies, the ambient concentration of N_2O is approximately 310 ppb V [2] (parts per billion (10^9) by volume). For continuous monitoring of N_2O in the atmosphere, a sensitivity in the 60-ppb V range may be needed. In order to distinguish N_2O from other pollutants, a molecule-selective technique, such as infrared absorption spectroscopy, must be employed.

To achieve the necessary sensitivity and selectivity, high-resolution laser techniques in the infrared (IR) and near-infrared (NIR) fingerprint regions can be applied. Therefore, the availability of tunable laser sources with suitable linewidths is essential for the further development of optical diagnostic techniques used in trace gas analysis. For practical applications, the main requirements for the light sources are small size, low weight and cost, narrow linewidth, large tuning range and no liquid nitrogen cooling.

✉ Fax: +49-6221/54-4255, E-mail: peter.hess@urz.uni-heidelberg.de

Recent developments in compact NIR and IR all-solid-state tunable lasers, such as tunable semiconductor lasers, quantum-cascade lasers and devices utilizing non-linear optical mixing in non-linear crystals (OPOs, difference frequency generators (DFGs), optical parametric amplifiers (OPAs)), have significantly advanced the application of optical absorption techniques in sensitive trace gas analysis. The optical techniques commonly employed are optical absorption spectroscopy with optical detection [3, 4], cavity-ringdown spectroscopy [5] and photoacoustic spectroscopy [6–9]. These techniques require tunable single-frequency lasers, such as distributed feedback (DFB) diode lasers or quantum-cascade lasers. Non-linear OPO, DFG or OPA devices can also be used, but the finite linewidth of such devices may reduce the selectivity and may significantly modify the absorption spectra of the measured species.

Usually, semiconductor lasers are operated in the continuous-wave (CW) mode. For spectroscopic applications, single-mode distributed-feedback (DFB) diode lasers should be applied. The main advantage of using DFB lasers is that they provide excellent selectivity for neighboring narrow absorption lines. Since these lasers can be easily modulated and have the potential for rapid wavelength scanning, the detection sensitivity can be enhanced by amplitude- or wavelength-modulation of the laser and lock-in amplification of the detector signal. Another possibility is to average many spectra recorded by rapid scans over a selected wavelength range. However, the widespread utilization of these lasers has been hindered by one or more of the following shortcomings: low power, limited continuous tuning range and stringent electronic and temperature control to maintain wavelength stability. For high sensitivity, the absorption path has to be increased and sophisticated detection methods (derivative spectroscopy, double-frequency modulation, etc.) have to be applied. This can be achieved only by complex and expensive systems. In the case of photoacoustic spectroscopy, the highest available laser power, additional acoustic resonance amplification and phase-sensitive lock-in signal processing are used to enhance the sensitivity.

For field applications under atmospheric conditions, the pressure-broadened linewidth of the detected species (0.1–0.3 cm^{-1}) reduces the significance of the ultra-narrow linewidth feature of these lasers. However, a larger continuous tuning range is needed to achieve the necessary spectral

selectivity in multicomponent mixtures. These requirements can be fulfilled by the above-mentioned tunable non-linear laser systems. Therefore, these laser sources currently play an increasing role in trace gas analysis [3, 10, 11].

A periodically poled lithium niobate (PPLN) OPO using a simple grazing-incidence grating cavity configuration (GIOPO) for broad and fast wavelength tuning has been developed [12] for the mid-infrared region. Depending on the power of the Nd:YAG pump laser, this GIOPO is capable of producing 20–120 mW of infrared power with a bandwidth of 0.2 cm^{-1} at 1–2 μm and of 0.8 cm^{-1} at 3 μm. Since pressure-broadened linewidths are in the range of a few tenths of a wavenumber, the GIOPO output bandwidth is suitable for exciting single well-separated rotational–vibrational absorption lines or Q-branch lines of many gases under typical atmospheric conditions. For example, the absorption spectrum of the asymmetric stretching vibration ν_3 of methane was measured recently with the GIOPO [13], and a separation of the methane lines from neighboring water lines was possible despite the finite linewidth of the GIOPO [14]. However, the rotational structure of the vibrational bands of heavier molecules (CO_2, N_2O, NO_2 etc.) cannot be resolved with this laser, because the separation of the rotational lines is much smaller for these molecules ($\sim 1\,cm^{-1}$) than for methane ($\sim 10\,cm^{-1}$).

Since the GIOPO is pumped by a laser-diode-pumped Q-switched Nd:YAG laser at several kilohertz (< 10 kHz) repetition rate, it is possible to match the repetition rate with the acoustic resonance frequency of a resonant photoacoustic cell. A differential PA detector [6] designed for sensitive PA spectroscopy has been combined with the GIOPO for sensitive gas analysis using the photoacoustic technique. In a previous experiment [13], the signal output of the GIOPO was used in combination with a single resonant cell to excite methane gas in the first overtone $2\nu_3$ in a nitrogen atmosphere, resulting in a detection sensitivity of 30 ppb V. In an improved experiment, the idler beam of the GIOPO was used to excite the fundamental ν_3 vibration and to measure the concentration of methane in ambient air in situ [14]. In these measurements, the sensitivity was increased to 1.2 ppb V due to the higher absorption coefficient of methane at 3 μm and an improved differential PA detector.

2 Experimental set-up

The experimental set-up is shown in Fig. 1. The GIOPO was similar to that described in [12], only the laser-diode-pumped Q-switched Nd:YAG laser had a smaller power (∼ 2 W) and the optical cavity was optimized for the idler output of the GIOPO. A PPLN crystal was pumped by the 1064-nm beam of the Nd:YAG laser. The front and rear surfaces of the crystal plate were antireflection coated for 1064 nm and the wavelength region of the idler beam. A 1064-nm filter and an antireflection-coated Ge filter were used to block the residual pump laser light and the signal output of the GIOPO, transmitting only the idler beam. The usable wavelength range of the idler was determined by the period of the poled region selected and the temperature of the PPLN crystal. The three PPLN crystals available, each with eight periodically poled regions, provided a total tunability range between 2.5 μm–4.5 μm. Continuous fine tuning of the idler wavelength over a range of approximately 15 cm^{-1} was performed by scanning the tuning mirror using a microstepping motor controlled by a PC. A larger scan range ($\sim 150\,cm^{-1}$) was obtained by a combination of temperature and stepping-motor tuning. The output power after the Ge filter was typically approximately 25 mW. A gold-coated copper mirror, with a radius of curvature of 406 mm, was used to focus the infrared beam into the resonator tube, which had an inside diameter of 5.5 mm and a length of 40 mm.

The differential PA detector employed was designed for fast time response, low electronic and acoustic noise and high sensitivity. The device had a fully symmetrical design, with dual acoustic resonator tubes sandwiched between two acoustic filters. A more detailed description of the PA detector can be found elsewhere [6]. The repetition rate of the pump laser at

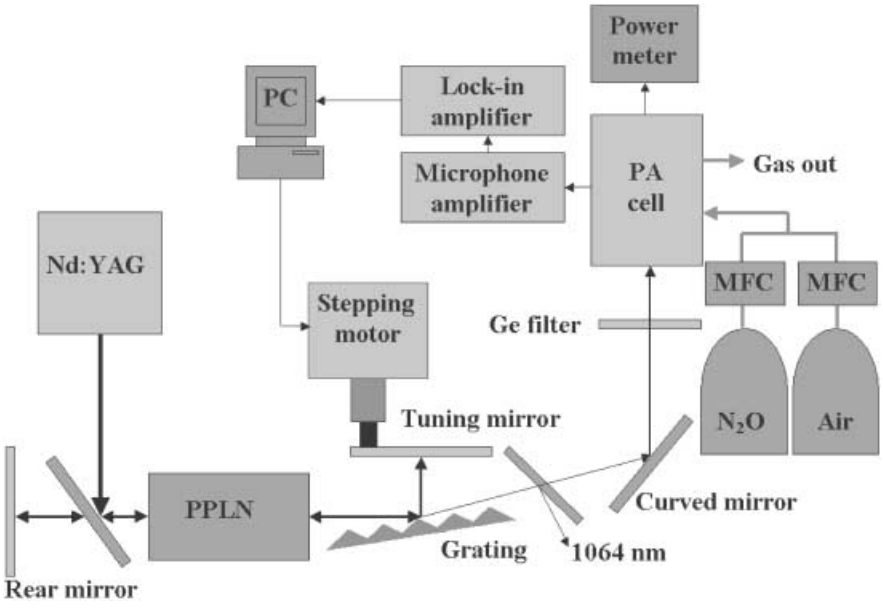

FIGURE 1 Set-up for photoacoustic trace gas measurements with the GIOPO as a light source

1064 nm was controlled by the internal reference signal of the lock-in. The frequency was adjusted to match the longitudinal acoustic resonance of the cell at approximately 4 kHz.

The preamplified photoacoustic signal was measured using a digital lock-in amplifier (Stanford model 830, time constant: 1 s) and recorded with a PC. The X and Y components of the lock-in output signal were normalized to the power of the infrared output of the GIOPO and plotted as a function of wavelength to obtain the PA spectrum.

All measurements were carried out at a gas flow rate of 200 sccm. A certified mixture of 50 ppmV N_2O in synthetic air was diluted by mixing with a stream of synthetic air. High-resolution mass flow controllers (MFCs, Tylan FC 260 series) were employed to control the gas flow. The volume flow of synthetic air was controlled by a 300 sccm MFC, while three different MFCs (50 sccm, 10 sccm and 1 sccm) were used to adjust the flow of the certified gas. The mass flow controllers were adjusted to maintain the total volume flow at 200 sccm.

3 Results and discussion

The measurements were performed in three steps. First, the wavelength range of the N_2O measurements was determined by using the HITRAN database [15]. The $(\nu_1 + \nu_3)$ combination band of the symmetric and asymmetric stretching mode between 3420 and 3510 cm^{-1} was selected for the PA measurements (Fig. 2a). The temperature of the PPLN crystal and the grating angle were selected in such a way that the idler output was centered close to 3492 cm^{-1} (2.864 μm) with maximum power. The differential PA cell was aligned for minimal background at 200-sccm synthetic air flow. The noise was measured by blocking the laser beam. First, the noise performance was checked with gas flow. The broadband intrinsic noise (measured with a broadband voltmeter) of the miniature electret microphones of 15–20 μV was relatively large. However, this noise was completely uncorrelated with the modulation frequency. The in-phase (N_X) and quadrature (N_Y) components of the noise measured by the lock-in were around 20 nV. These values depended on the time constant of the lock-in. Theoretically, N_X and N_Y should become approximately zero with increasing time constant. This tendency could be observed in the present measurements. In contrast, the fluctuations of the noise components were quite stable. Therefore, the standard deviations of the noise components (time constant 1 s) were regarded as the N_X and N_Y components of the noise. The values of N_X and N_Y were around 60 nV in all experiments. The B_X and B_Y components of the background signal measured for synthetic air were about thirty-times larger (~ 2 μV). Since the background and the noise should be added as uncorrelated quantities, the sum of B_X and N_X is given as $\sqrt{B_X^2 + N_X^2}$, the contribution of the noise to the background and to the PA signal can be neglected.

The second step was the measurement of the absorption spectrum of N_2O. A certified mixture of 50 ppmV N_2O in synthetic air was made to flow through the PA cell while the GIOPO was tuned over the selected spectral range by applying combined temperature and stepping-motor tuning. The measured PA spectrum of the $(\nu_1 + \nu_3)$ band is shown in Fig. 2b. This spectrum was compared to simulated spectra obtained by convolving the HITRAN spectrum with Gaussian lineshapes with different full-width at half-maximum (FWHM) values. Best agreement was found for a Gaussian lineshape with 0.4 cm^{-1} FWHM. The relevant parts of the convolved HITRAN spectrum and the measured PA spectrum are shown in Fig. 3a and b. Since the measured and calculated spectra are almost identical, the FWHM of the idler can be regarded as being approximately 0.4 cm^{-1}, about half the value of the idler linewidth in the previous methane measurements (~ 0.8 cm^{-1}) [14]. This result shows that the optimization of the optical cavity for the idler wavelength and the reduction of the internal losses within the optical cavity by antireflection coatings ensures a linewidth that is narrow enough to resolve the rotational structure of several important trace gases under atmospheric conditions.

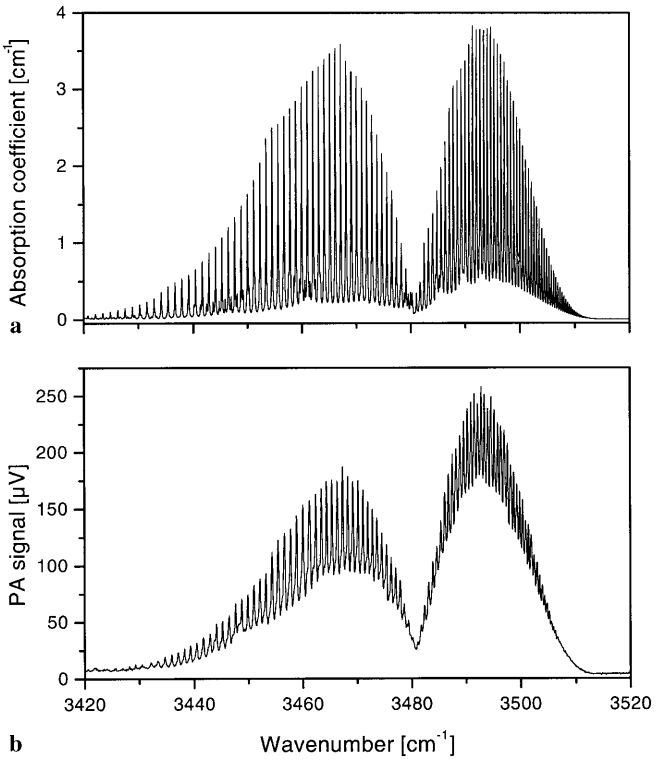

FIGURE 2 **a** HITRAN spectrum of the $(\nu_1 + \nu_3)$ combination band of 1% N_2O in synthetic air. The absorbance was calculated for a 100-cm path length. **b** The measured PA spectrum of the whole band

Due to the finite linewidth of the GIOPO, the effective absorption coefficient was smaller than the value given by HITRAN modeling. The value of the maximal absorption coefficient at 3492 cm^{-1} is 3.87 cm^{-1} according to HITRAN and about 1.65 cm^{-1} for the convoluted spectrum. Thus, the effective absorption coefficient of N_2O was estimated to reach only about 45% of the HITRAN value.

The sensitivity of the GIOPO-PA system for N_2O was determined by calibration measurements. The idler wavelength was set to the center of the peak at 3492 cm^{-1} and the GIOPO power was optimized by adjusting both the grating and the PPLN-crystal temperature.

Three calibration measurements were carried out. The concentration of N_2O was reduced from 7500 ppb V to 350 ppb V in 6 steps (MFC 50), from 2500 ppb V to 40 ppb V in 11 steps (MFC 10) and from 225 ppb V to 20 ppb V in 6 steps (MFC 1). The errors involved in the concentrations

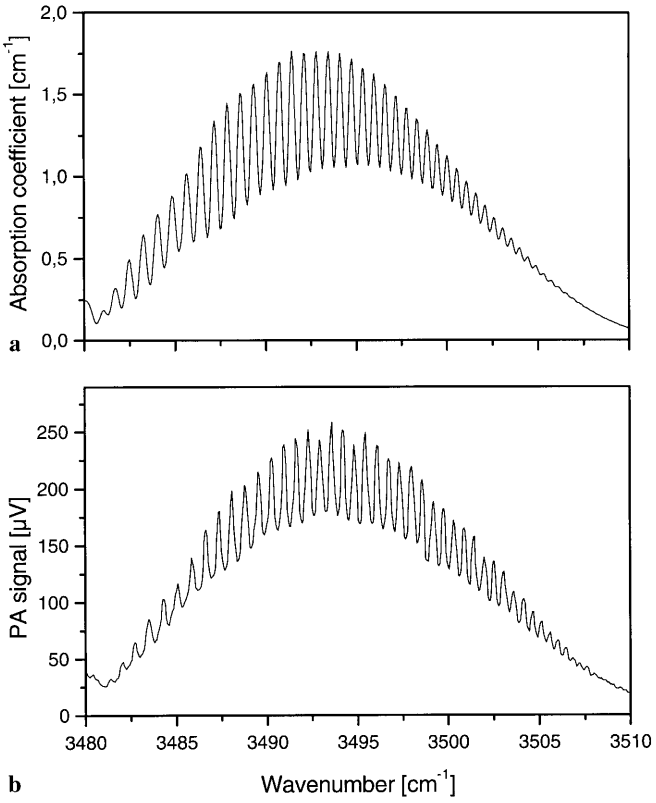

FIGURE 3 **a** Convolution of a 0.4 cm^{-1} broad Gaussian lineshape (FWHM) and the HITRAN spectrum of Fig. 2a. **b** The measured PA spectrum

could be determined from the errors of the mass flow controllers (2% of the full range). Since the absolute error of the MFCs was constant, the relative error increased drastically for low settings of the MFCs. Therefore, the error in the concentration approached 100% at the lowest settings of the three MFCs.

The in-phase (U_X) and quadrature (U_Y) components of the preamplified microphone signal were measured by the lock-in. The corresponding components of the background (B_X, B_Y) were determined in a pure flow of synthetic air, while the N_X and N_Y components of the flow, acoustic and electromagnetic noise were obtained by blocking the laser beam. The X and Y outputs of the lock-in and the output of the light power meter (W_L) were read out and stored by the LabView program. Altogether, 3×50 data values were collected at each concentration setting. The mean values of these data blocks were regarded as the measured U_X, U_Y and W_L values at the corresponding concentration, while the standard deviations (σ) of these data were regarded as the errors of the measured U_X, U_Y and W_L values. The measured U_X and U_Y lock-in amplitudes were normalized to 25-mW light power (the average power during the three calibration measurements), in order to find comparable values. The standard deviations of the light power data were below 0.5 mW ($\sim 2\%$).

Since the background is usually coherent with the laser light, i.e. it has quite a stable phase lag of Θ_{BG} to the lock-in reference, and the true PA signal S has a different but constant phase lag Θ_{PA}, both quantities can be regarded as vectors with components:

$$\begin{aligned} S_X &= S\cos\theta_{\mathrm{PA}} \qquad S_Y = S\sin\theta_{\mathrm{PA}} \\ B_X &= B\cos\theta_{\mathrm{BG}} \qquad B_X = B\sin\theta_{\mathrm{BG}} \end{aligned} \tag{1}$$

The components of the measured microphone signal U can then be considered as sums of the corresponding S and B components. Taking into account that the PA signal S is strictly linear [6, 9] with the concentration w, that is, $S = aw$, both U_X and U_Y must be linear functions of the concentration:

$$\begin{aligned} U_X &= a_X w + B_X \\ U_Y &= a_Y w + B_Y \end{aligned} \tag{2}$$

where a_X and a_Y are the X and Y components of the photoacoustic sensitivity (given in μV/ppb V).

It follows from (2) that the absolute magnitude U of the measured PA signal is not a linear function of the concentration [9, 14]. Therefore, the usual method of evaluation of PA measurements, i.e. fitting a linear function to the measured (U, w) data pairs, may give a smaller slope than the true one. Therefore it is preferable to evaluate the U_X and U_Y data points separately.

The calibration measurements were evaluated in the following way. The S_X and S_Y components of the PA signal were determined by subtracting the measured background component B_k from the corresponding microphone signal components U_k. This procedure was carried out for each calibration measurement. Then straight lines through the origin were fitted to the entire set of corrected data points of both vector components $S_k = U_k – B_k$. The fit parameters a_k provide the components of the sensitivity vector a. The absolute value of a, calculated from the a_X and a_Y components, can be regarded as the sensitivity of the photoacoustic N_2O detector.

The sensitivities determined by the fit were $a_X = 0.00313 \pm 0.00001$ μV/ppb V and $a_Y = 0.00243 \pm 0.00001$ μV/ppb V. The calculated PA sensitivity was $a = 0.00405 \pm 0.00001$ μV/ppb V. The measured PA amplitudes $\sqrt{(U_X - B_X)^2 + (U_Y - B_Y)^2}$ and the calculated linear PA signal $S = aw$ are shown in Fig. 4. The errors in the PA signal and concentration are shown as error bars for each data point. The lower sensitivity limit can be defined as the concentration at which the PA signal is equal to the noise. Since both noise components are around 60 nV, the lower sensitivity limit ($SNR = 1$) can be estimated as 20 ppb V. This sensitivity limit, however, could not be realized in mixing experiments. Although gas mixtures with nominal concentrations of 20, 30 and 40 ppb V were mixed by the gas mixing system and PA measurements were performed, the mixing error in the concentration exceeded 100% at these low concentrations. Therefore, the lowest measurable concentration should be defined by $SNR = 3$. In this case, the lower limit will be approximately 60 ppb V. As can be seen in Fig. 4, both the signal and concentration errors are then smaller than 50%.

Since the PA signal is proportional to the product of the light power and absorption coefficient, the sensitivity of the detector itself can be estimated by multiplying together the GIOPO power, the actual absorption coefficient (Fig. 3) and the lower concentration limit: $D = 0.025\,\mathrm{W} \times 1.65\,\mathrm{cm}^{-1} \times 60 \times 10^{-9} \cong 2.5 \times 10^{-9}\,\mathrm{W\,cm}^{-1}$. The result is

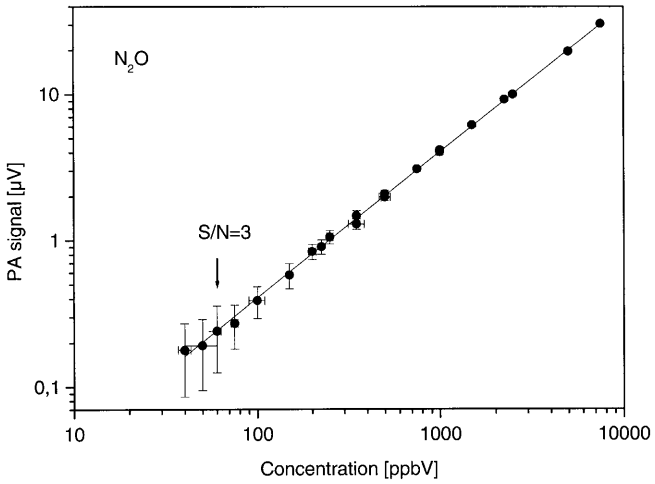

FIGURE 4 Calibration curve of photoacoustic N_2O detection. *Dots*, measured and background-corrected PA signal; *line*, linear fit

somewhat larger than the previously published sensitivity of the same differential PA detector of $1.4 \times 10^{-9}\,\mathrm{W\,cm^{-1}}$, which, however, was derived for $SNR = 1$ [14].

The linear concentration dependence of the PA signal and the known behavior of the background facilitate the calibration of the PA detector for a given species. It is sufficient to measure the X and Y components of the microphone signal U and background B and to calculate the PA signal amplitude as $S = \sqrt{(U_X - B_X)^2 + (U_Y - B_Y)^2}$ of a certified gas mixture of concentration c. The photoacoustic sensitivity can be determined as $a = S/c$. In order to reduce the error caused by the uncertainty in the concentration, of course, it is better to use three calibrated mixtures with different concentrations and to calculate the photoacoustic sensitivity as the arithmetic average of the three individual a values.

Unknown concentrations of a given gas can be obtained by calculating the photoacoustic amplitude S from the measured U and B values, and by dividing S by the value of a determined by the simple method described above.

4 Conclusion

It has been demonstrated that the spectral resolution of a GIOPO–PA system is sufficient to resolve the rotational structure of the $(\nu_1 + \nu_3)$ combination band of N_2O. According to the HITRAN spectrum of Fig. 2, the separation of the individual lines around $3492\,\mathrm{cm^{-1}}$ is only 0.6–$0.7\,\mathrm{cm^{-1}}$. These lines are well separated in the measured PA spectrum (see Figs. 2b and 3b). Since lines separated by $0.5\,\mathrm{cm^{-1}}$ around $3505\,\mathrm{cm^{-1}}$ could also be resolved, the spectral resolution of the set-up was better than $0.5\,\mathrm{cm^{-1}}$.

The lower limit of the sensitivity of the N_2O concentration measurements at $SNR = 3$ was 60 ppb V. The actual limitation was given by the accuracy of the mixing procedure. The sensitivity achieved could be sufficient for continuous monitoring of N_2O in the atmosphere, if the interference with water vapor can be sufficiently reduced. By taking into account the value of the absorption coefficient of N_2O, the absorption coefficient still measurable by the PA set-up can be given as $\alpha_{\min} = 1 \times 10^{-7}\,\mathrm{cm^{-1}}$. The detector sensitivity D defined as the product of the GIOPO idler power of 0.025 W and the minimum absorption coefficient is given as $D = 2.5 \times 10^{-9}\,\mathrm{W\,cm^{-1}}$. The values of both $\alpha_{\min}$ and D agree reasonably well with our previous results obtained for methane and ammonia.

ACKNOWLEDGEMENTS We thank A.H. Kung and his coworkers for their continuous help with setting up the GIOPO. Financial support of this work within the bilateral scientific cooperation project between Germany (DAAD) and Taiwan (NSC) is gratefully acknowledged.

REFERENCES

1 J. Kaiser: Science **294**, 1268 (2001)
2 M.W. Sigrist (Ed.): *Air Monitoring by Spectroscopic Techniques* (Wiley, New York 1994)
3 D. Richter, D.G. Lancaster, F.K. Tittel: Appl. Opt. **39**, 4444 (2000)
4 A.A. Kosterev, R.F. Curl, F.K. Tittel, C. Gmachl, F. Capasso, D.L. Sivco, J.N. Baillargeon, A.L. Hutchinson, A.Y. Cho: Opt. Lett. **24**, 1762 (1999)
5 A.A. Kosterev, A.L. Malinovsky, F.K. Tittel, C. Gmachl, F. Capasso, D.L. Sivco, J.N. Baillargeon, A.L. Hutchinson, A.Y. Cho: Appl. Opt. **40**, 5522 (2001)
6 A. Miklós, P. Hess, Z. Bozoki: Rev. Sci. Instrum. **72**, 1937 (2001)
7 B.A. Paldus, T.G. Spence, R.N. Zare, J. Oomens, F.J.M. Harren, D.H. Parker, C. Gmachl, F. Capasso, D.L. Sivco, J.N. Baillargeon, A.L. Hutchinson, A.Y. Cho: Opt. Lett. **24**, 178 (1999)
8 J. Sneider, Z. Bozóki, A. Miklós, Z.S. Bor, G. Szabó: Int. J. Environ. Anal. Chem. **3**, 1 (1997)
9 A. Schmohl, A. Miklós, P. Hess: Appl. Opt. **41**, 1815 (2002)
10 K. Kuhnemann, K. Schneider, A. Hecker, A.A.E. Martis, W. Urban, S. Schiller, J. Mlynek: Appl. Phys. B **66**, 741 (1998)
11 C. Fischer, M.W. Sigrist, Q. Yu, M. Seiter: Opt. Lett. **26**, 1609 (2001)
12 C.S. Yu, A.H. Kung: J. Opt. Soc. Am. B **16**, 2233 (1999)
13 G.C. Liang, H.H. Liu, A.H. Kung, Á. Mohácsi, A. Miklós, P. Hess: J. Phys. Chem. A **104**, 10 179 (2000)
14 A. Miklos, C.H. Lim, W.W. Hsiang, G.C. Liang, A.H. Kung, A. Schmohl, P. Hess: Appl. Opt. **41**, 2985 (2002)
15 http://www.hitran.com